Simulation of transient flow in microhydraulic pipe system

Kamil Urbanowicz[1][0000-0001-9226-2053] Michał Stosiak[2][0000-0002-6111-1332]

Krzysztof Towarnicki[2][0000-0002-4881-2548] Huan-Feng Duan[3][0000-0002-9200-904X]

Anton Bergant[4][0000-0002-7872-9665]

[1] West Pomeranian University of Technology, Szczecin, Faculty of Mechanical Engineering and Mechatronics, Szczecin, Poland, kamil.urbanowicz@zut.edu.pl
[2] Wrocław University of Science and Technology, Faculty of Mechanical Engineering, Department of Technical Systems operation, Wrocław, Poland, michal.stosiak@pwr.edu.pl, krzysztof.towarnicki@pwr.edu.pl
[3] Dept. of Civil and Environment Engineering, Hong Kong Polytechnic Univ., Hung Hom, Kowloon, Hong Kong, hf.duan@polyu.edu.hk
[4]Faculty of Mechanical Engineering, University of Ljubljana, Slovenia

Abstract. This paper presents the modeling and simulation of transient in microhydraulic pipe systems. Liquid stream energy dissipation occurs mainly as a result of friction losses. Theoretical considerations of water hammer resulting from rapid valve closing, supported by experimental verification, were undertaken. The experimental system incorporated a straight two-meter section of a steel pipe with an internal diameter of 4 mm. An attempt was made to determine the degree of conformity of the water hammer model (previously verified in conventional pipes) to the experimental results obtained for small-internal-diameter pipes. Shear stress on the pipe wall was modelled using first a simplified quasi-steady approach and then an effective modified unsteady friction model. The pressure waveforms at the valve (at the end of the pipe) were obtained for initial flow velocity, v_{01}= 2,39 m/s and v_{02}=1,14 m/s respectively. Experimental studies were carried out in the region of laminar flows with Reynolds numbers below 100.

Keywords: water hammer, wall shear stress, microhydraulic pipe, modelling, testing, method of characteristics, unsteady friction.

1 Introduction

Unsteady flows occur commonly in hydraulic, water supply and transmission systems as well as in living organisms (circulatory systems) [1-4]. Because of the wave character of flow disturbance propagation, they pose a considerable danger to complex systems with many branches (water supply and hydraulic systems) since waves superposition can occur in these systems [5]. In hydraulic systems (hydraulic machines, motor vehicles, etc.), where distribution blocks are commonly used, each change-over of the devices can lead to unsteadiness. The high pressures accompanying such states can

cause leaks and in extreme cases (bursts) they can lead to the total destruction of the overloaded system components [6]. Therefore, elements protecting such systems are commonly employed [7]. But they considerably increase the planned costs of the systems. In order to avoid these costs, it is necessary to better identify the behaviour of such systems under an unsteady load. This knowledge will help to optimize the choice of system components. Mathematical models describing flows with acceptable accuracy can be used for this purpose. The models which enjoy increasing popularity are characterized by essential simplicity, whereby they can be simply applied to any considered system. The group of such models includes 1D models having a highly simplified structure [8]. One can use them to calculate (in close to real time) changes in two basic flow parameters, i.e. flow rate (the mean flow velocity in the cross section) and pressure, in the particular cross-sections of the analysed systems. Such a model was used in this study to simulate water hammer. Since in the experiments the change-over time of the directional control valve affected the pressure fluctuation time, the mathematical model was adapted by introducing a modified boundary condition in the directional control valve location.

2 Test stand

An abrupt closure of the flow in a hydraulic conduit results in an instantaneous pressure rise in the hydraulic line. In order to determine the effect of a microhydraulic system change-over the test stand shown in Fig. 1 was built.

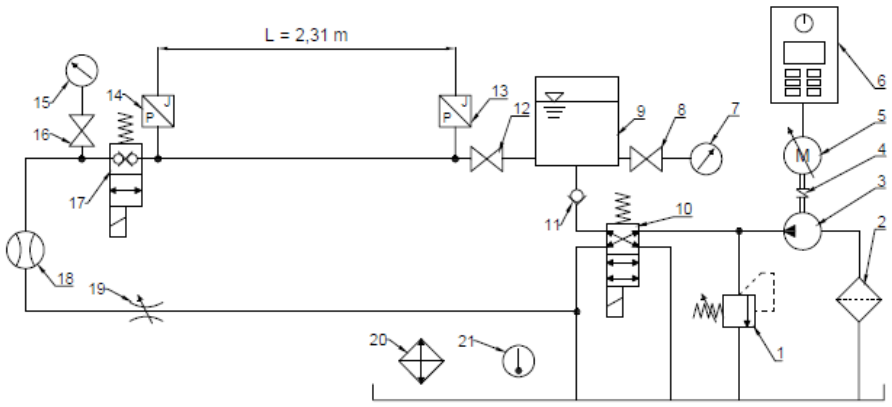

Fig. 1. Schematic of tests stand: Schematic of hydraulic measuring system: 1 – safety valve, 2 – suction filter, 3 – displacement gear pump, 4 – flexible coupling, 5 – electric drive motor, 6 – power supply box with built-in frequency converter, 7 – pressure gauge, 8 – cut-off valve, 9 – accumulator , 10 – 4/2 slide valve controlled by electromagnetic coil, 11 – non-return valve, 12 – cut-off valve, 13,14 – pressure transducer, 15 – pressure gauge, 16 – cut-off valve, 17 – cut-off valve controlled by electromagnetic coil, 18 – flowmeter, 19 – throttle valve, 20 – cooler, 21 – thermometer.

A steel hydraulic pipe with an outer diameter of 0.006 [m] and an inner diameter of 0.004 [m] is the principal test stand member constituting the basis for the mathematical model. AT-5230 pressure transducers (13) and (14) were installed on the pipe's ends (one on each of the ends) to measure pressure in it. The pressure transducers can measure pressure up to max. 250 [bar]. A CASAPA PLP 10.1D0 external gear pump (3), with a unit delivery of 1 [cm^3/rotation], was used to generate liquid flow and pressure. A PARKER HANNIFIN GS27300NSOL CART VALV cut-off valve (17) was installed on the pipe's end to rapidly close the flow through the pipe. The valve's closing element is controlled by the coil of a conventional PARKER HANNIFIN 14W 24VDC-CCS024 D magnet (acc. to the manufacturer specifications, the leakage from the valve amounts to 33 [cm^3/min]). After the cut-off valve a pressure gauge (15) coupled with a manually controlled cut-off valve (16) was installed. In the vicinity of the pressure gauge a BADGER METER BM-OG FLOW METER IND OG-1/4"-S-S-1-V-LF flowmeter (with measuring accuracy $\pm 5\%$ of the mean value) was installed to measure the rate of flow in the pipe. A pre-set throttle valve (19) was connected to the flowmeter's outlet to obtain the mean pressure in the investigated hydraulic line. A flexible hydraulic conduit with an inner diameter of 0.004 [m] was connected to the throttle valve whereby the liquid was transported back to the tank. The hydraulic power unit had the form of a cuboid whose top plate was secured with screws. A pump was fixed to the bottom of the plate in such a way that its housing was partially immersed in the liquid. A suction filter (2) was installed on the pump's inlet port to ensure the proper filtration of the working liquid. A T-connection was installed on the pump's outlet pump, whereby a single-stage safety valve (1) could be installed in parallel to the main delivery line to reduce pressure that could damage the pump's displacement parts. Further on the main delivery line a conventionally electrically controlled VSE 4/2/B-14/1 distributor valve (10) was connected in series. Its function was to change the direction of the liquid flow generated by the pump at the instant when the flow was closed by the cut-off valve situated at the pipe's end. A non-return valve (11) was installed to prevent the flow of the liquid along the section from the distributor valve (10) to the investigated flow at the instant of distributor change-over. A hydraulic accumulator (9) was installed after the non-return valve on the main supply line. The accumulator had the form of a cylindrical tank with a capacity of 13 [dm^3]. For system servicing purposes a cut-off valve (12) was placed between the accumulator and the investigated pipe. On the other side, at the connection of the investigated pipe, a pressure gauge (7) and a cut-off valve (8) were installed to measure mean pressure in the accumulator (9). The accumulator's supply connection was made on its bottom axis. The hydraulic system was equipped with a thermometer (21) and a cooler (20) – a basic system temperature stabilization component. Other cooling system components were fans mounted on the cooler's side wall and a controller for switching them on. Owing to the system's thermal inertia and the temperature stabilization component the set temperature could be attained with an accuracy of ± 2 [°C]. The assumed water hammer could be produced by simultaneously changing over the cut-off valve (17) and the distributor valve (10) The electromagnetic coils whose function was to control the above elements were connected in parallel to the electric power supply unit. Owing to this solution the elements could be changed over at the same time. The pump was driven by connecting its drive shaft to an electric

motor's shaft by means of a coupling. The motor was supplied from a frequency converter (6) enabling the stepless change of the rotational speed of the motor's drive shaft. The signals registered by the tensometric pressure sensors (13) and (14) were transmitted through screened conductors (eliminating disturbances) to a Tektronix TDS-224 digital oscilloscope coupled with a computer equipped with an AD/DA card and the Wave Star-Tektronix software. Each of the tensometric pressure sensors was equipped with a dedicated signal amplifier and was supplied from a dedicated feeder incorporating an over-current protection circuit. The investigated hydraulic conduit was immovably fixed to a foundation insulated from ambient vibrations. The distance between the pressure measuring points (pressure sensors) was L = 2.31 [m], the velocity of sound propagation – c = 1180 [m/s], the dynamic viscosity of the liquid in the system – $\nu = 1 \cdot 10^{-4}$ $[m^2/s]$ (determined according to ASTM D7042), the density of the oil – $\rho = 869$ $[kg/m^3]$ (determined according to ISO 12185) and the temperature of the oil during the experiments – $T = 20$ [℃]. Mineral oil was the medium used during the measurements. In order to precisely determine the viscosity and density of the working liquid at the set temperature during the measurements a sample of the oil was sent to a specialist laboratory. The laboratory tests conclusively showed that oil ISO32 was the oil used in the experiments.

3 Mathematical model

The unsteady flow in pressure conduits is described in this paper by the system of basic equations [8] of continuity (1) and motion (2):

$$\frac{\partial p}{\partial t} + c^2 \rho \frac{\partial v}{\partial x} = 0 \tag{1}$$

$$\frac{\partial v}{\partial t} + \frac{1}{\rho}\frac{\partial p}{\partial x} + \frac{2\tau}{\rho R} = 0 \tag{2}$$

where:
v=v(x,t) – the mean velocity of the liquid in the pipe cross section,
p=p(x,t) – the pressure in the pipe cross section,
R – the inner diameter of the pipe,
τ – the wall shear stress,
ρ – the density of the liquid,
g – the acceleration due to gravity,
c– the pressure wave velocity,
t – time,
x – the axial coordinate of the pipe.

The wall shear stress τ is a function of the mean flow velocity and its derivative $\tau = \tau\left(v, \frac{\partial v}{\partial t}\right)$ [9]:

$$\tau = \frac{f\rho}{8} v|v| + \frac{2\mu}{R}\int_0^t w(t-u) \cdot \frac{\partial v(u)}{\partial t} du \tag{3}$$

The first term of the above equation represents a quasi-steady quantity in which f is the Darcy-Weisbach friction factor. The second term, which is a convolution integral, represents a time dependent quantity in which $w(t-u)$ is the so-called weighting function. In this paper the convolution integral was solved in an effective manner using the Urbanowicz's solution [10]:

$$\tau_{(t+\Delta t)} = \frac{\rho f_{(t+\Delta t)}}{8} v_{(t+\Delta t)} \left| v_{(t+\Delta t)} \right| + \frac{2\mu}{R} \sum_{i=1}^{3} \underbrace{\left[A_i y_{i,(t)} + \eta B_i \left[v_{(t+\Delta t)} - v_{(t)} \right] + C_i [1-\eta] \left[v_{(t)} - v_{(t-\Delta t)} \right] \right]}_{y_{i,(t+\Delta t)}} \tag{4}$$

Coefficients A_i, B_i, C_i and weighting function correction factor η are calculated from the formulas discussed in detail in paper [10]. The fact that the above relation currently consists of only three expressions is the result of the filtration of the effective weighting functions used in the calculations. Details of this filtration are discussed in paper [11].

3.1 Boundary condition

Since the distributor change-over was not instantaneous, the pressure inside the distributor during the change-over will be calculated here similarly as for slow valve closing. As opposed to the formulas found in the literature [8, 12, 13], the formulas presented below were derived for the basic flow parameters, i.e. averaged flow and pressure velocities.

During a change-over one may calculate the instantaneous velocity value at $t < T_c$ using the method of characteristics and the following formula:

$$v_{(1,t)} = \frac{0.5 c\rho\theta^2 {v_{(1,t=0)}}^2}{p_{(1,t=0)}} - \sqrt{\left(\frac{0.5 c\rho\theta^2 {v_{(1,t=0)}}^2}{p_{(1,t=0)}} \right)^2 + \frac{c\rho\theta^2 {v_{(1,t=0)}}^2}{p_{(1,t=0)}} \left(\frac{p_{(2,t-\Delta t)}}{c\rho} - v_{(2,t-\Delta t)} + \frac{4\Delta t \tau_{(2,t-\Delta t)}}{\rho D} \right)} \tag{5}$$

After calculating the above value inside the distributor valve one can then determine the pressure prevailing in the same place from the following relation:

$$p_{(1,t)} = c\rho \left(v_{(1,t)} - v_{(2,t-\Delta t)} \right) + p_{(2,t-\Delta t)} + \frac{2c\Delta t \tau_{(2,t-\Delta t)}}{R} \tag{6}$$

In the above formulas the characteristic of the distributor valve being closed is modelled by time function $\theta(t)$. In this paper the following form of this function was assumed:

$$\theta = 1 - \left(\frac{t}{T_c} \right)^2 \tag{7}$$

The shape of the function is shown in Fig. 2.

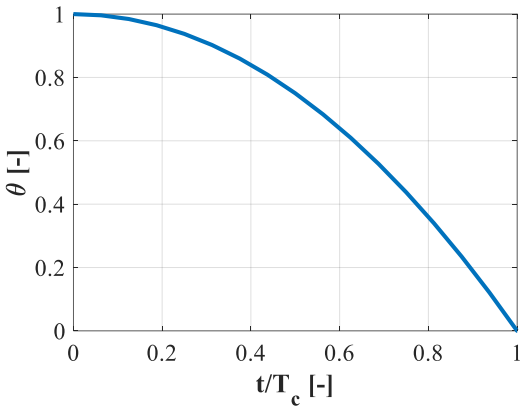

Fig. 2 Hydraulic valve closure relation characteristic.

4 Simulation results

For the purposes of this study a series of experiments were carried out on the test stand described in details in Fig. 1. The Oil ISO32 was the liquid flowing in the analysed hydraulic system. The tests were conducted on 12.11.2019. During the tests the temperature inside the hydraulic system increased slightly from 19 to 21 Celsius degrees. The change in temperature affected the values of the two key mathematical model parameters: viscosity and density (responsible for, i.e., the simulated hydraulic resistance), whose detailed values are presented in Table 1.

The method of characteristics (MOC) was used to solve the system of partial differential equations (1) and (2) presented in section 3. This numerical method interprets well the physical nature of the unsteady flow and is characterized by quick convergence, the ease of taking different boundary conditions into account, and a high accuracy of the calculation results. Using it one can solve the analysed system of equations in a simple way. The solution consists of finding an equivalent system of four ordinary differential equations, which is then solved by means of finite differences. Approximation with first-order differential schemes yields satisfactory results. The detailed solution can be found in [10]. The calculated pressure wave velocity in this short pipe ($L = 2.31\ [m]$) was $c = 1180\ [^{m}/_{s}]$. In all the investigations presented below the conduit was discretized into $N = 16\ [-]$ elements (the number of reaches in the numerical calculation). This axial discretization guaranteed the fulfilment of the computational compliance criteria [14] and forced the following time step $\Delta t = 1.22 \cdot 10^{-4}\ [s]$. All the other parameters needed for simulations are contained in Table 1. Selected results of the tests are presented in Figs 3 and 4 below, where the experimental results (the broken line) are compared with the simulation results (the solid line). For each of the investigated flows the simulation results were obtained in four ways:

a) by rapidly (instantaneously) changing over the distributor valve ($T_c < \Delta t$) – hydraulic resistance calculated in the quasi-steady way (denoted as IC+QSF);

b) by spreading the change-over of the distributor valve over time (the change-over time in these conditions was determined to amount to $T_c = \frac{L}{c} = \frac{2.31}{1180} = 1.96 \cdot 10^{-3}\ [s]$, i.e. to one fourth of the full water hammer period) – hydraulic resistance calculated in the quasi-steady way (denoted as RC+QSF);

c) by rapidly (instantaneously) changing over the distributor valve – hydraulic resistance calculated using the unsteady model (denoted as IC+UF);

d) by spreading the change-over of the distributor valve over time – unsteady resistance (denoted as RC+U).

For clarity, the abbreviations used in the above four cases and following figures stand for: IC – instantaneous closing time, QSF – quasi-steady friction, UF – unsteady friction, RC – real closing time.

Table 1. Parameters of analysed flows.

Case	Q_{dm} $[dm^3/\text{min}]$	Q $[m^3/s]$	v_0 [m/s]	Re $[-]$	p_R $[MPa]$	ρ $[kg/m^3]$	ν $[m^2/s]$	T [°C]
C01	1.801	3.00·10-5	2.39	86.86	5.25	870	1.1e^{-4}	19
C02	0.862	1.437·10-5	1.14	45.73	5.00	869	1e^{-4}	20

a)

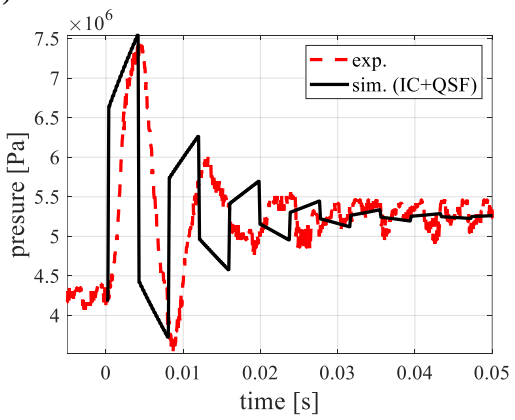

b)

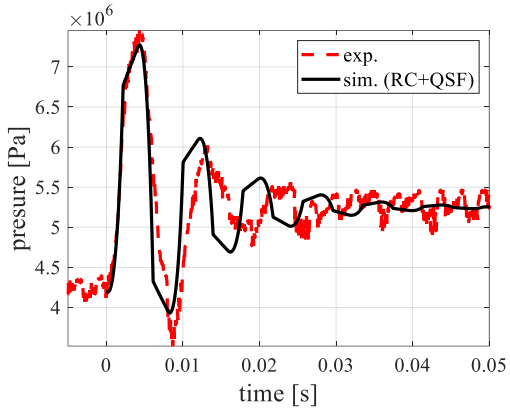

c)

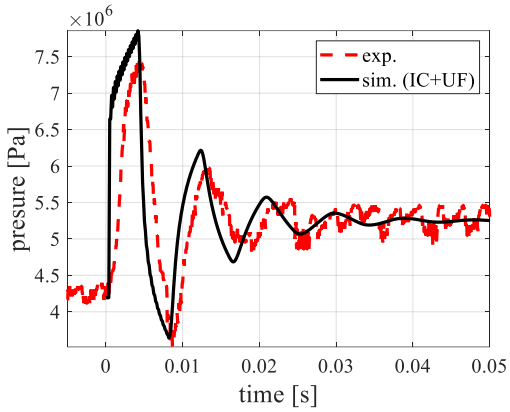

d)

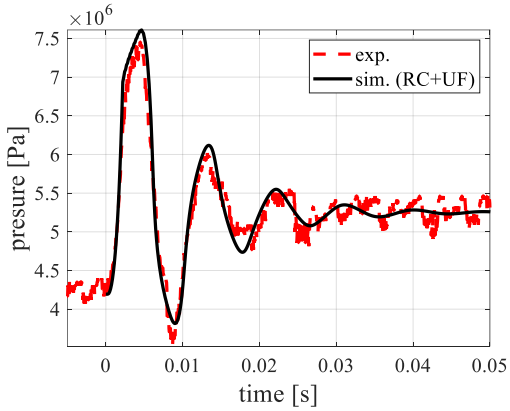

Fig. 3. Pressure variation in case C01 ($v_{01} = 2.39\ m/s$).

The comparisons for case C01 (characterized by the highest initial velocity) clearly indicate the effect of unsteady friction and the boundary condition (real closing) on the modelled graphs. Both the boundary condition and unsteady friction may indirectly affect the duration of the successive pressure amplitudes. When RC and UF are used, this duration will be extended. Owing to this, when considering the effect of unsteady friction, the simulation conformity can be regarded as satisfactory (Fig. 3d). As shown in Fig. 3a, the use of only quasi-steady resistance with a rapid instantaneous change-over of the distributor can result in a simulation graph significantly different from the real one. The misfit is most visible for the first amplitude, where the experimental graph gradually increases until it reaches its maximum value (t=0.005 [s]), and then gradually decreases over time until it reaches its minimum at t=0.009 [s]. Whereas in the case of the simulated graph, the pressure rise and drop are instantaneous and out of phase (e.g. the sharp pressure drop at t=0.005 [s]). These figures show that the device registering pressure jumps (the pressure sensor) captured the first three amplitudes. The next amplitudes are not visible in the graph, which is due to the high noisiness of the experimental results performed in this microhydraulic pipeline system.

a)

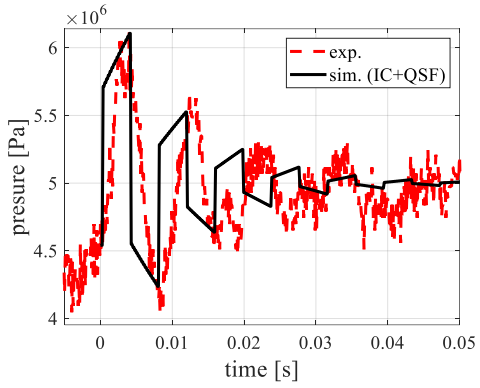

b)

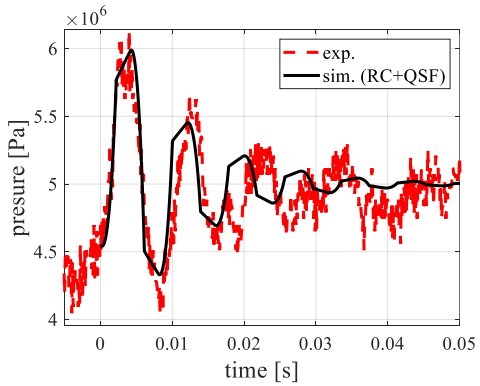

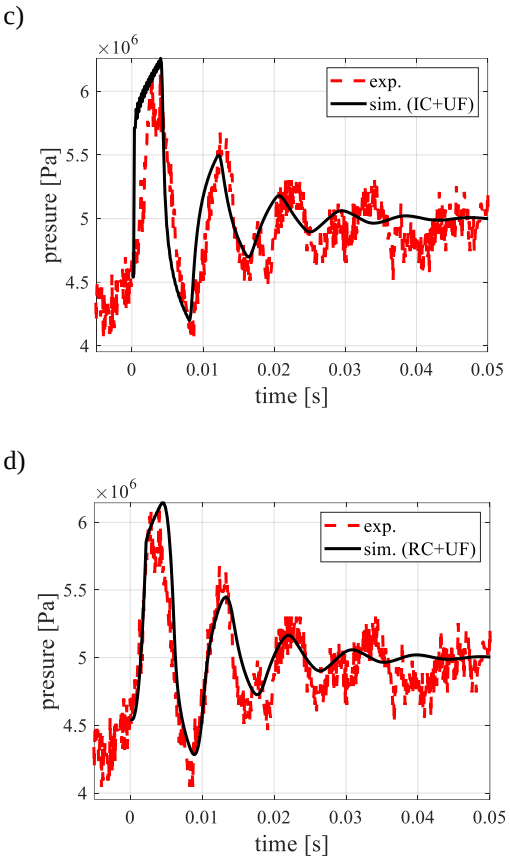

Fig. 4. Pressure variation in case C02 ($v_{02} = 1.14\ m/s$).

The second case, i.e. C02, was characterized by relatively low flow rate $v_{02} = 1.14\ [^{m}/_{s}]$ that has a lower Reynolds number than former case C01. Similarly, the measurement noise is also significant at this rate. Fortunately, the first three pressure amplitudes were correctly registered, while the next amplitudes are very noisy. Meanwhile, the use of solely the quasi-steady model approach (Fig. 4a) can result in significant discrepancies (e.g., the third amplitude is modelled in counterphase) and that the use of a correct boundary condition (described by equations (5)-(7)) coupled with unsteady friction (Fig. 4d) would be able to provide better fit of the simulated result to the experimental one. Furthermore, the comparison of results in Fig. 3 and Fig. 4 demonstrates that the system and measurement noises can provide more significant influence in case C02 than case C01, which indicates the resistance of initial Reynolds number flow state to the influence of system and measurement noises (i.e., noise tolerance).

Summing up, the comparisons of these two cases show that:

- in microscale conduits, in which the closing time of the flow cutting off element (a valve, a distributor, a slide, etc.) is greater or equal to ¼ of the water hammer period $T_c \geq L/c$, the effect of this closure can be regarded as significant;

- when considering the real valve closing time in the modeling, this has a significant effect on the results of simulations (the shape of the modelled graphs is consistent with that of the experimental graphs);

- in the case of such microscale conduit sections, it is recommended to take unsteady friction into account since it also has an important influence on the final shape of the modelled amplitudes (e.g., comparing Fig. 3b and Fig. 4b (RC+QSF) with the results obtained using the model presented in this paper – Fig. 3d and Fig. 4d (RC+UF));

- the conventional model, commonly used to simulate flows in pipes with inner diameter D > 10 [mm], is also suitable for modelling water hammers in pipes with relatively small diameters $D \leq 4$ [mm] (usually regarded as microtubes [15, 16]).

5 Conclusions

Numerous comparative investigations were carried out as part of this research on the water hammer in a micro-hydraulic pipeline system. The experimental results were compared with the numerical results obtained by solving the basic equations describing one-dimensionally the unsteady flow.

The selected results of the comparative investigations have revealed the important role which the correct modelling of the flow cutting-off device closing characteristic (close to the real one) plays in such microscale conduits when a simple water hammer ($T_c \leq \frac{2L}{c}$) occurs in them. In real systems, valve closing, or as is the case here the distributor change-over, never is instantaneous. The results and analysis have shown that the closing (change-over) time is of key importance in this kind of systems. The modified numerical method [10, 11] has been confirmed to be effective in predicting transient states in such systems (short pipe sections and very small inner diameters).

As next step work, the investigations will be continued with applying the other fluid (oil ISO10) that has much lower viscosity, so as to further verify the developed model as well as to examine the effects of temperatures on different fluids in microhydraulic pipe systems.

References

1. Karadzić U., Janković M., Strunjas F., Bergant A.: Water Hammer and Column Separation Induced by Simultaneous and Delayed Closure of Two Valves, Strojniški vestnik. Journal of Mechanical Engineering 64(9), 525-535 (2018).
2. Iffa R.B., Triki A.: Assessment of inline technique-based water hammer control strategy in water supply systems. Journal of Water Supply: Research and Technology-Aqua 68(7), 562–572 (2019).

3. Jiang D., Lu Q., Liu Y., Zhao D.: Study on Pressure Transients in Low Pressure Water-Hydraulic Pipelines. IEEE Access 7, 80561-80569 (2019).
4. Mei C.C., Jing H.: Effects of thin plaque on blood hammer—An asymptotic theory. European Journal of Mechanics - B/Fluids 69, 62-75 (2018).
5. Jung B.S., Karney B.: A practical overview of unsteady pipe flow modelling: from physics to numerical solutions. Urban Water Journal 08, 502-508 (2016).
6. Stosiak M.: The impact of hydraulic systems on the human being and the environment, Journal of Theoretical and Applied Mechanics 53(2), 409-420 (2015).
7. Moghaddas S.M.J., Samani H.M.V., Haghighi A.: Transient protection optimization of pipelines using air-chamber and air-inlet valves. KSCE Journal of Civil Engineering 21, 1991–1997 (2017).
8. Wylie E.B., Streeter V.L.: Fluid Transients in Systems. Prentice-Hall Inc., Englewood Cliffs, New Jersey (1993).
9. Zielke W.: Frequency-dependent friction in transient pipe flow. ASME J. Basic Eng. 90, 109 – 115 (1968).
10. Urbanowicz, K.: Fast and accurate modelling of frictional transient pipe flow. Journal of Applied Mathematics and Mechanics 98(5), 802 – 823 (2018).
11. Urbanowicz K.: Analytical expressions for effective weighting functions used during simulations of water hammer. Journal of Theoretical and Applied Mechanics 55(3), 1029-1040 (2017).
12. Pérez-Sánchez M., López-Jiménez A.P., Ramos H.M.: PATs Operating in Water Networks under Unsteady Flow Conditions. Control Valve Manoeuvre and Overspeed Effect, Water 10, 529 (2018).
13. Jensen R.K., Larsen J.K, Lassen K.L., Mandø M., Andreasen A.: Implementation and Validation of a Free Open Source 1D Water Hammer Code. Fluids 3(3), 64 (2018).
14. Urbanowicz K.: Computational compliance criteria in water hammer modelling. In: Wzorek M., Królczyk G., Król A. International Conference Energy, Enviromental and Material Systems (EEMS 2017) E3S Web Conf. vol. 19, pp. 302-315 . E3S Web of Conferences, Polanica-Zdrój (2017)
15. Vekariya P.B., Subbaiah R., Mashru H.H.: Hydraulics of microtube emitters: a dimensional analysis approach. Irrig Sci 29, 341–350 (2011).
16. Haifeng Ji, Huajun Li, Zhiyao Huang, Baoliang Wang, Haiqing Li: Measurement of Gas-Liquid Two-Phase Flow in Micro-Pipes by a Capacitance Sensor. Sensors 14, 22431-22446 (2014).